

DETECTION OF PHYTOGEOGRAPHIC INDICATORS WITH REMOTE SENSING AND GEOARCHAEOLOGY FOR DEVELOPMENT OF A LONG-TERM CLIMATE MONITORING STATION IN ISRAEL

Neil Manspeizer^{1*}, Amon Karnieli¹

¹Remote Sensing Laboratory, Blaustein Institutes for Desert Research, Ben Gurion University of the Negev, Sede Boker Campus 84990, Israel - (neilm@post.bgu.ac.il, akarnieli@bgu.ac.il).

KEY WORDS: geoarchaeology, remote sensing, vegetation dynamics, climate monitoring, Mediterranean, UN SDG 13

ABSTRACT:

The Mediterranean basin is a strong candidate for monitoring climate change successfully, a priority of UN SDG 13, because of its long settlement history. Human-environmental contact has typically hindered monitoring efforts because the natural indicators that enable dependable monitoring have been altered anthropogenically. This research describes a two-step process which turns that synanthropism into an advantage through geoarchaeology, remote sensing, GIS, meteorology, and floristic classification. First, archaeological survey data were employed in a semi-arid region of Israel to identify areas of more and less intensive land-use over 2300 years. Trend surfaces were derived in GIS from ancient periods of most intense monoculture agriculture (Hellenistic, Byzantine, and Ottoman). 2020 land-cover was classified using VENUS satellite wet / dry season NDVI imagery and an airborne LiDAR canopy height model. This was reclassified after fieldwork to three broad land-cover classes and cross-tabulated with the 2300-year land-use intensity model in GIS. The results indicate a land-use legacy whereby woody perennial species are more abundant where land-use was cumulatively less intense. Second, unmanned aerial vehicle surveys were conducted in these areas of less-intense land-use. There, on lightly grazed lands where woody encroachment occurs but chamaephytes regenerate due to the grazing, microplots were established. Phanerophyte and chamaephyte shrubs were identified based on Raunkiaer type and the species associated with chorotype (geographic origin). This was compared with aridity index values derived for the study area between 2010-2022. The study provides a prototype, using dependable phytogeographic indicators, that may be developed into a long-term climate monitoring station (LTCMS).

1. INTRODUCTION

One difficulty of challenging received wisdoms (Leach and Mearns, 1996) in this post-colonial period is establishing tools to develop new knowledge sets. That is true for climate science, especially regarding the decentralization of climate change data. Tools that enable nations to autonomously monitor climate change help the UN to achieve sustainability development goals (SDG) by promoting self-reliance and regional stability. The result is replicable science which utilizes remote sensing to develop knowledge sets from within the decentralized context (Ostrom, 2001). This paper addresses UN SDG goal 13 (climate change) through explanation of a prototype long-term climate monitoring station (LTCMS). The LTCMS, as a knowledge development tool, aims toward participatory development goals with a methodology that is transferable technologically. Climate monitoring would be ongoing under the SDG umbrella with data sharing through an "open access" data repository. The key lies in correct identification of the phytogeographic indicators of climate change within their anthropogenic-natural setting which is rigorous in scope. Typically, human disturbance is viewed as detrimental to use of phytogeographic indicators of climate change because the landscape has been altered. That is indicative of a well-known discussion in the literature concerning succession and dynamics of Mediterranean garrigue and maquis vegetation following disturbance (e.g., Giourga et al., 1998). The research presented here, as a methods paper, promotes the opposite idea, namely that anthropogenic activity associated with land-use (LU) can assist in identification of phytogeographic indicators for climate change monitoring.

The method incorporates utilization of synanthropic shrub-land vegetation, or flora developed in proximity to human activity, as indicators. That is accomplished by focusing geographically on

two types of disturbance along the synanthropic axis: (1) long-term agricultural LU intensity that causes variable land-cover (LC) patterns due to differential primary and secondary succession of synanthropic vegetation following abandonment (Manspeizer and Karnieli, 2023); and (2) short term disturbance of woody perennial succession through a proximate cause, such as grazing, that promotes "arrested succession" of woody encroachment (Manspeizer, 2006) but also enables regeneration of sub-shrub species. That two-stage process of disturbance along the synanthropic axis is typical of many semi-arid rangelands in the Mediterranean because of the long human settlement history. Of the twenty-two countries around the Mediterranean basin, 15% of their total land area was considered permanent meadow or pasture in 2020 (FAO, 2023) which represents a potentially large-scale system to monitor climates. This synanthropic window between natural and human-disturbed landscapes in shrub-lands requires a multi-disciplinary approach for study: (1) archaeological survey data are developed into a geographic information systems (GIS) database and used to identify areas of more and less intensive LU over a long-term period; (2) comparison of current land-cover (LC), derived from remotely sensed imagery, with GIS derived LU intensity; and (3) areas of less intense long-term LU that demonstrate arrested succession from a proximate cause, such as light grazing, are focused upon for climate change study through species level shrub mapping.

At an even larger scale, semi-arid lands account for approximately 15% of the earth's land surface and are comprised of agricultural areas defined as rainfed, cropland and rangeland for almost 1/3 of the world's population (United Nations, 2011). Utilization of the Mediterranean basin as a prototype for how other semi-arid regions can monitor climate change represents an

* Corresponding author

innovative use of rangelands and the potential to develop a global database. The hypothesis for the study is based on previous works in botany that describe phanerophyte shrub and chamaephyte sub-shrub presence along gradients related to climate such as elevation and temperature (Di Biase et al., 2021; Schmiedel et al., 2012). Climate related gradients can help to distinguish between plants based on physiological adaptations (Liphschitz and Lev-Yadun, 1986) and life forms (Danin and Orshan, 1990). For example, phanerophytes are associated with the moister part of the precipitation gradient and more semi-arid phytogeography. Chamaephytes, on the other hand, are associated with the drier part of the precipitation gradient and more arid phytogeography (Keshet et al., 1990; Margaris et al., 1992). The prototype LTCMS presented in this paper deals with climate gradients by correlating shrub life-form presence across geographic zones, for example from arid to semi-arid to sub-humid. In this manner, the chorotypes associated with species compositions in place may be associated with the convergence of climate systems reflected in local aridity. Therefore, shrubs as phytogeographic indicators can be monitored for significant changes to community composition to help define climate regimes and their changes.

1.1 Case Study: Maresha Hinterland

The best method to demonstrate this approach is a case study developed in the southern Judean foothills, Israel. Previous fieldwork describes that landscape as a Mediterranean phanerophyte maquis matrix with inter-space Mediterranean and Irano-Turanian chamaephytes associated with garrigue, hard-rock, and shrub-steppe habitats (Manspeizer and Karnieli, 2021). The area of study¹ lies in the hinterland south of *Tel Maresha*² (archaeological mound). The area is rich in settlement history with a wealth of material cultural remains in the landscape. Today, 96.7% of the hills in the study area lie within an overlapping military zone / nature reserve with light cattle grazing (for definitions see Kirk et al., 2019), which accounts for its character as "open space". The study area is also part of the foothills ecological corridor in Israel that connects the southern Negev Desert with the northern Galilee Mountains west of the Judean Mountains to promote wildlife migration and plant dispersal. Antiquities Authority (IAA) survey data were incorporated into a GIS database and cross-tabulated with a LC classification from 2020 to determine areas of more and less intense long-term LU. Second, unmanned aerial vehicle (UAV) surveys were conducted in areas of less-intense long-term LU, namely the Gad Hills nature reserve. There, on lightly grazed lands, where woody encroachment occurs and phytogeographic shrub indicators may regenerate, all woody perennials including phanerophyte and chamaephyte were mapped. These shrubs were classified according to percent presence of chorotypes and compared with the aridity index (AI) values between 2010–2022 derived from regional potential evapotranspiration (PET).

The three periods of most intensive ancient monoculture agriculture were chosen to represent major anthropogenic disturbance at the landscape scale. The location of Hellenistic oil presses, Byzantine winepresses, and Ottoman animal pens, were developed into a GIS database from IAA survey data (Dagan, 2006). Archaeological excavations at *Tel Maresha* and its hinterland to the south, revealed a large-scale olive oil industry from the Hellenistic period (333–63 BCE) in the study area then known as northern Idumea. Twenty-seven 'Maresha type' industrial-scale olive oil presses were found at *Tel Maresha* and another fifteen / sixteen at sites in the hinterland (Kloner and

Sagiv, 1989). Based on the number and size of oil presses, estimates indicate that 450 mt of olive oil, or 500,000 l, could have been produced annually by northern Idumea. That would have required between 100,800–262,500 olive trees in the 42 km² study area based on sixteen to twenty-five olive trees per 0.4 ha (Vossen, 2007). During the Byzantine period (324–640 CE), a vast rural Christian population inhabited the study area. The agricultural change included a leap from thirty-seven winepresses found with Roman period pottery to 183 winepresses with Byzantine period pottery which conforms to descriptions of industrial scale viticulture in Byzantine period Palaestina. Based on ancient methods of viticulture (Weber, 2009), the volume of wine capable of being produced in the study area during the Byzantine period is 2667 mt at 2 t of grapes per ha and 230 l of wine per ton of grapes. During the Ottoman period (1516–1917 CE) there is significant archaeological evidence of renewed LU after nearly a millenia of secondary succession during the Early Muslim and Medieval periods (640–1516 CE). Remains of several pastoralist movements were identifiable within the archaeological survey including twenty-six Ottoman period animal pens found in the study area (Dagan, 2006). Based on an average 9.5x7.5 m per pen and two-three sheep or goats per 1 m², average carrying capacity of the study area was between 3705 to 5558 animals/yr (USDA, 2006). The LU history is essential to understanding the current LC and while topographic effects, associated with aspect, elevation, or soil type, are evident in the landscape they do not describe the most dominant landscape scale vegetation pattern. That is best described as a LU legacy (Foster et al., 2003) in which disturbances, such as long-term ancient agricultural LU, have affected the substrate causing a significant discernable modern LC.

Questions in the literature regarding Mediterranean vegetation dynamics concentrate on whether LC patterns are driven by anthropogenic or natural factors. For example, anthropogenic stress will initially in the short-term cause an increase in annual cover that is replaced by shrub species (Giourga et al., 1998: 589–596). The case study presented here was established to help answer these questions through juxtaposition of the two drivers. Results of the initial research (Manspeizer and Karnieli, 2021) demonstrate the LU legacy which contributes to the debate on Mediterranean vegetation. That study stated that long-term anthropogenic stresses, as demonstrated through the archaeological survey work, drives a more dominant long-term LC state than described in previous literature. However, this left questions regarding the role of climate and other environmental factors that were described in more detail in a second study (Manspeizer and Karnieli, 2023). There, it was clarified, following UAV vegetation mapping, that anthropogenic stresses do produce different LC patterns of the same floristic association (phytogeographic state) given continuity in climate regime. Thus, Tzanopoulos et al. (2005: 27–38) write that maquis species are replaced by sub-shrub species if certain thresholds of anthropogenic use are exceeded. However, in addition to synanthropic relations, changes in climate regime were hypothesized to also drive changes in floristic composition. Monitoring climate change could therefore be accomplished through the LTCMS, especially with use of remote sensing methods to detect appropriate phytogeographic indicators. This paper offers an empirical approach to deconstruct the shrub composition and the temporal aspects of climate change (variability / fluctuation) as they relate to the phanerophyte maquis matrix compared with the chamaephyte garrigue.

¹ 42 km² rectangle centered at Lat. 31.54135, Long. 34.88722

² *Tel Maresha* was inscribed a UNESCO world heritage site in 2014.

2. ANALYSIS

2.1 Data and Methodology

The methodology comprised two stages: (1) LU/LC analysis with geoarchaeology, remote sensing and GIS to isolate less-anthropogenically influenced vegetation within the synanthropic gradient; and (2) climate analysis based on vegetation mapping in less-intensely used areas and species correlation with chorotype and climate variables. Four materials were assembled within a database used for the fieldwork and analysis: (1) Israel Antiquities Authority (IAA) archaeological survey data for ancient land-use; (2) Remotely sensed data (VEN μ S spaceborne, LiDAR airborne, and UAV for land-cover; (3) climate related data from the Israel Meteorological Service (IMS) and US Department of Energy (DOE); and (4) field survey for floristic classification and literature review of the floristic association

2.1.2 LU/LC Analysis was comprised of land-use and land-cover components with IAA archaeological data and 2020 remotely sensed land-cover classification. The IAA survey of the study area, conducted between 1982-1986 by Dagan (2006), included the Amazyra and Lakhish sheets (1:20000 scale). The survey maps contain information organized as 'sites' where archaeological remains were found based on the maximalist approach. The IAA surveyors described the material remains (e.g., pottery, agricultural installations, building stones) that were identified and recorded according to location and historical periodization. In the study area were 124 relevant archaeological survey sites on the Amazyra sheet and 72 on the Lakhish sheet. Sites were categorized based upon: (1) type of remains, such as settlement, farmstead, building(s), and agricultural installations (presses, terraces and kilns); and (2) pottery scatter per period associated with each find. 196 IAA survey sites in that study area were digitized and stratified in the GIS database according to the relevant findings between the Hellenistic and Ottoman periods.

The three ancient periods of most intensive monoculture agriculture were chosen to represent major historical anthropogenic disturbance. This decision was based on the agricultural extensification visible in the material culture remains. Associated installations, namely subterranean Hellenistic oil presses, rock-hewn surface Byzantine winepresses, and stone construction Ottoman animal pens, were digitized in GIS as point files from the IAA survey data. Distance images from the agricultural installations for each of the three periods were derived. A reciprocal of the distance image was derived to represent land-production pressure in proximity to installation. These images were stretched between 0-255 such that a buffer around the installation reflected an impact that decreased along a gradient as distance increased. This notion has been described in range ecology literature for grazing impacts around pens or watering holes (Sasaki et al., 2008). A ninth-order polynomial surface trend image was derived from the distance images and stretched again (0-255) for each period. The three stretched trend images were then averaged into one image that describes the cumulative land-use intensity over 2300 years.

2020 land-cover data were derived from two sources: (1) spaceborne Vegetation and Environment monitoring New Micro Satellite (VEN μ S) imagery; (2) airborne Light Detection and Ranging (LiDAR) imagery. Two 2020 VEN μ S satellite images of the study area were acquired with 10 m spatial resolution that represent vegetation peak (March) following the wet winter season in the Mediterranean region and vegetation trough (September) following the dry summer season. Red (666.2 nm

center) and Near Infrared (861.1 nm center) bands were chosen, and the two dates analyzed using the normalized difference vegetation index (NDVI). NDVI, a sum-difference ratio, has been used to discern vegetation from bare soil areas studies and assist study of seasonal differences in vegetation cover (Karnieli, 2003; Karnieli et al., 2002).

$$\text{NDVI} = (\text{NIR-Red}) / (\text{NIR+Red}) \quad (1)$$

LiDAR is an active laser system that detects canopy height and topographical differences with high spatial resolution. The two common LiDAR data products are the Digital Terrain Model (DTM) that represents elevation and the Digital Surface Model (DSM) that provides the height of the vegetation at each point. The LiDAR data was acquired between February 2015 and July 2016 at 1 m spatial resolution. The DSM was smoothed (DSMs) and the DTM subtracted to create a normalized Digital Surface Model (nDSM), i.e., the vegetation height.

$$\text{nDSM} = \text{DSMs} - \text{DTM} \quad (2)$$

The nDSM image and two NDVI images from March and September 2020 were used as three bands in an unsupervised LC classification with TerrSet (2017). The resulting classification, with fifteen classes based on spectral reflectance and canopy height, was used to ground-truth the LC in situ at the end of the rainy season (March 2021). Twenty-two points were chosen to ground-truth the classification and the fifteen classes were reclassified into three vegetation classes: bare, shrub, and tree.

The intermediate output of the GIS work was one model of ancient LU intensity and one model of 2020 LC. GIS analysis was standardized spatially between LU / LC at 1 m resolution. All alluvial areas, territory in the Palestinian Authority, and a high-power line were masked which left the hills of the study area. The trend surface image, 2300 years average cumulative LU intensity, was stretched as an integer binary image to 255 classes. The lowest (0-92) and highest (207-255) levels of LU intensity contained no assignments as they occurred in the masked areas. Crosstabulation, a GIS method of a database query, was conducted between the cumulative trend image and 2020 LC. Spatial crosstabulation, a statistical tool to compare categorical data sets, allows each new category to represent the original data sets. All old pixel categories are preserved in the analysis and re-sorted into new combined categories such that each new pixel has two old values (LU intensity and vegetation class). The results of the crosstabulation reflect the range of values between 92-207 on 55% of the image or 19.8 sq km within the hills of the study area.

2.1.3 Climate Analysis was conducted in Gad Hills Nature Reserve, after the LU/LC analysis determined that the reserve corresponded with less intensely used land based on archaeological data³. Four plots in the hills were selected based on stratified-random sampling that contained garrigue / maquis communities only rather than species related to the tributaries. Aerial surveys were flown at the end of the winter wet season during NDVI peak between April 10 – May 7, 2022 (Karnieli, 2003). Four microplots in each plot were photographed at nadir from a height of 50 m using the DJI mini2 UAV and autonomous flight plans in Litchi App. Ground sample distance (GSD) was calculated at 1.82 cm based on flight height, focal length, and fields of view (FOV). All aerial photos were georeferenced in QGIS (2022) with 0.125m georeferenced orthophotos from the Survey of Israel. Twenty ground control points were established for each multiplot with average residual (RMS) error of 15.56

³ Israel National Nature and Parks Authority Permit #043-2022

which translates to an average 28.31 cm on the ground (GSD * RMS error) for the four plots.

The goal was to map percent presence of shrub species and the UAV photos assisted only in the detailed digitization of the vegetation data. Two microplots were chosen from each of four plots (eight total) and all woody vegetation within were mapped over the wet season 2022-2023. The final percent presence included only phanerophyte shrubs and chamaephyte sub-shrubs that were not also climbers or parasites. In all 13411m² was surveyed in the eight microplots and the coverage checked through GPS tracking. Chamaephyte regeneration due to wet season changes was accounted for by fieldwork conducted three different times between December 2022 – February 2023. The published Ceratonia-Pistacia lentisci typicum association that describes the regional area was first developed by Zohary and Orshan (1959: 288-290). It was cross-referenced with the online database by Danin and Fragman-Sapir (2016) to build a "published cross-referenced association" of potential shrub species along with their chorotypes (region of origin) and habitat.

Specific temperature and precipitation data do not exist for the study area so seven nearby meteorological stations (Kiryat Gat, Kibbutz Halamed'hay, Lehavim, Dorot, Negba, Shani and Rosh Tzurim) were used to provide a proxy. The climate data for the seven stations was established from two sources, the IMS climate archive data (I.M.S., 2023) and the DOE solar position calculator (SOLPOS, 2023). Potential evapotranspiration (PET_{HS}) based on Hargreaves-Samani (Almorox and Grieser, 2016) was derived between 2010-2022 as the climate variables were existent for all seven stations during that period (3). AI values were then derived from precipitation and PET_{HS} (4) for the seven stations.

$$PET_{HS} = 0.135 * KT * (T_{av} + 17.8) * (T_{max} - T_{min})^{0.5} * R_a * d \quad (3)$$

where $KT = 0.17$ (coefficient default)

T_{av} = Average Temp / day (C°),

$T_{max/min}$ = Temp / day (C°)

R_a = Extraterrestrial solar radiation in mm/d

d = number days in each iteration (1 = daily)

Avg PET / day (mm day⁻¹)

AI is calculated as:

$$AI = P / PET_{HS} \quad (4)$$

where P = Precipitation / yr (mm)

GIS analysis was used to develop AI surfaces between 2010-2022 at the meteorological stations. The surfaces were interpolated at 10 m spatial resolution for the 7 points using TerrSet (2017) with no six-point radius to smooth the results. AI for the study area specifically was derived from the interpolated surfaces (2010-2022). Aridity was compared with the chorotypes of shrub species identified and the chorotype zones as mapped previously by Danin and Orshan (1999: 16). A more precise representation of the relationship between aridity and chorotype would reflect shifting chorotype contours as vegetation compositions changed due to climate variability and fluctuation. That is beyond the scope of this paper, therefore a functional representation was derived by extracting statistical values from the AI surfaces in GIS between 2010-2022 for the two chorotypes found there. Chorotype shift, a reflection of the climate changes evident in the vegetation composition, may be expressed statistically as a range between: (1) max study area AI value minus min chorotype one AI value; and (2) min study area AI value minus max chorotype two AI value.

$$R : \{(AI_{S^*A_MIN} - AI_{CH1_MAX}), (AI_{S^*A_MAX} - AI_{CH2_MIN})\} \quad (5)$$

where R = Range of chorotype shift in study area

$AI_{S^*A_MAX/MIN}$ = max/min AI value (Study Area)

AI_{CH1_MAX} = chorotype one min AI value (M-IT)

AI_{CH2_MIN} = chorotype two max AI value (M)

This representation enables research along a gradient as conditions move between favorable and unfavorable over time relative to chorotype and species (sect. 3.5).

3. RESULTS AND DISCUSSION

Results of the study are limited to: (1) LC classification in 2020; (2) LULCC crosstabulation; (3) Climate analysis; (4) UAV vegetation mapping; and (4) Phytogeographic-Climatic correlation.

3.1 Land-cover Classification

The 2020 classification used VENμS NDVI seasonal imagery and vegetation height from the LiDAR nDSM. That classification described fifteen distinct spectral classes and three vegetation covers: (1) five classes of low annual cover between 0.09 to 0.13 m; (2) five classes of shrub between 0.10 to 2.42 m; and (3) five classes of tree species from 5.5 to 7.2 m. The masked 2020 classification included 56% annuals (grasses and flowers) and bare areas (rocky), 43% shrubs, and 1% trees.

3.2 Land-use Legacy

Cumulative LU intensity was crosstabulated with the 2020 LC images using a hard GIS crosstabulation. After normalization, the crosstabulation indicates that areas of least intense LU contained proportionally higher ratios of shrub and tree cover in 2020 than areas of most intense LU that contained higher ratios of bare regions in 2020. The results demonstrate that anthropogenic disturbance produces long-term LC effects identifiable in garrigue and maquis communities that are not due to topographic effects. That was reported previously in detail (Manspeizer and Karnieli, 2021, 2023), concurs with dominant theories in disturbance ecology (White and Jentsch, 2001), and demonstrates a LU legacy (Foster et al., 2003).

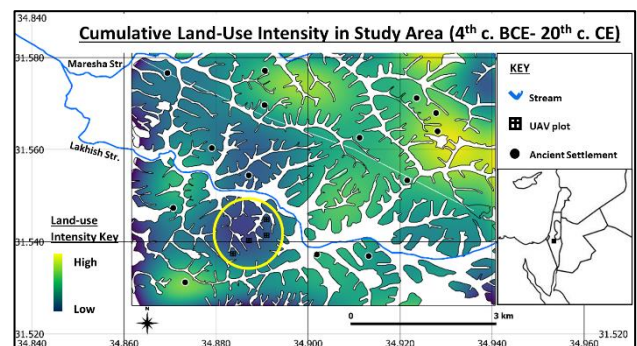


Figure 1. 2300 years cumulative land-use intensity in the study area from trend analysis with major ancient settlements and location of UAV vegetation plots in Gad Hills reserve circled.

3.3 Climate Analysis

The climate classification model for this paper is constructed around the aridity index derived from P and PET_{HS} calculations. Like Koppen-Trewartha (KT), it is based on: (1) climate analysis of meteorological variables (precipitation, solar irradiance and temperature); and (2) vegetation compositions with associated species chorotypes. This classification process requires several steps to utilize phytogeographic indicators of climate change, namely: (a) development of aridity indices over time; (b) shrub

species and chorotype mapping; and (c) ultimately development of a chorotype based atmospheric circulation model (future goal). In step one, regional AI were developed from PET_{HS} data. Figure 2 shows AI of the seven meteorological stations and study area according to the 12-year period of recorded data (2010-2022). The non-normal distribution of data demonstrates the seasonal conditions described by Raunkiaer as favorable or unfavorable (Danin and Orshan, 1990). For example, the study area is defined as semi-arid (0.2-0.5) based on the results, although in 2010-2011 and 2016-2017 the AI dipped into arid conditions (<0.2). This alone is insufficient to declare whether the conditions are favorable or unfavorable phytogeographically without inclusion of chorotype regions which is a spatial exercise.

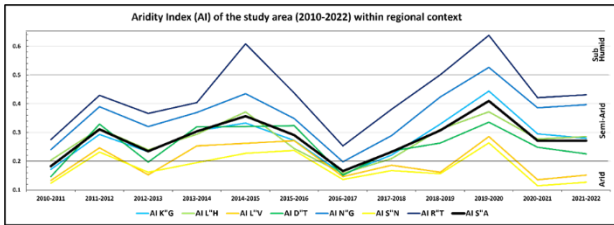


Figure 2. AI of the study region between 2010-2022 (Sources: I.M.S., 2023; SOLPOS, 2023). The seven stations are Kiryat Gat (K'G), Kibbutz Halamed'Hay (L'H), Lehavim (L'V), Dorot (D'T), Negba (N'G), Shani (S'N) and Rosh Tzurim (R'T). The Study Area (S'A) is depicted in thick black line.

Therefore, GIS interpolation was used to develop AI surfaces between 2010-2022 based on variables at the seven meteorological stations so that could be compared spatially with chorotype region. The shifting AI between 2010-2022 of the study region, evident in figure 2 as non-normal data trends, are viewed as interpolated surfaces in figure 3. Chorotype contours were digitized from phytogeographic maps published by Danin and Orshan (1999: 16) so that they may be associated with the aridity index surfaces. The chorotypes include Mediterranean (M), Irano-Turanian (IT), and Saharo-Arabian (SA) but may often described as a combination between them. The southern Levant is a convergence zone between these three large chorotype regions and locally that convergence demonstrates itself in mixed spatial zones. One goal of the larger project is to understand the percent presence of shrub indicators as related to chorotype in order to redefine these mixed zones and regions as they change over time due to climate change.

The chorotype contours in figure 3 do not reflect any change over the 12 year period and were initially derived in 1987 following a significant mapping effort (Danin and Orshan, 1999). A more ideal representation would reflect shifting chorotype contours because they would represent changes in species composition due to changing climate conditions. That necessitates a more elaborate project, such as the proposed LTCMS, however a provisional method is described in section 3.5. Statistics derived from chorotype regions based on the AI are correlated so the current conditions may be understood relative to favorable / unfavorable. Figure 3 is significant because it is a visual representation of the climate classification system demonstrating both meteorological variables and chorotypes. On its own, that method would suffice as a beginning climate classification systems akin to KT. However the vegetation mapping is necessary to relate the shifting chorotypes, phytogeographic indicators and aridity with climate changes. In that way, chorotype regions, defined by the vegetation that comprises them, may be linked with the climate conditions. To that end, sections 3.4 and 3.5 describe how UAV vegetation mapping may be linked to chorotypes and associated meteorological variables.

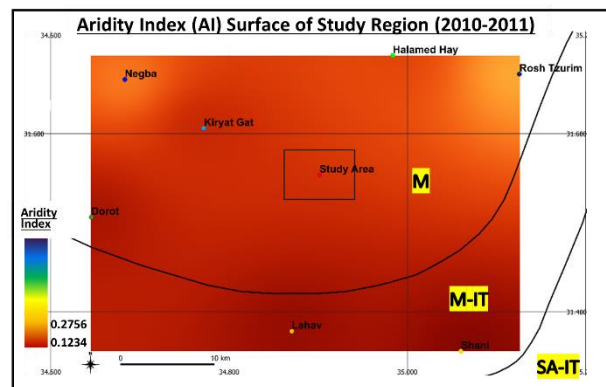
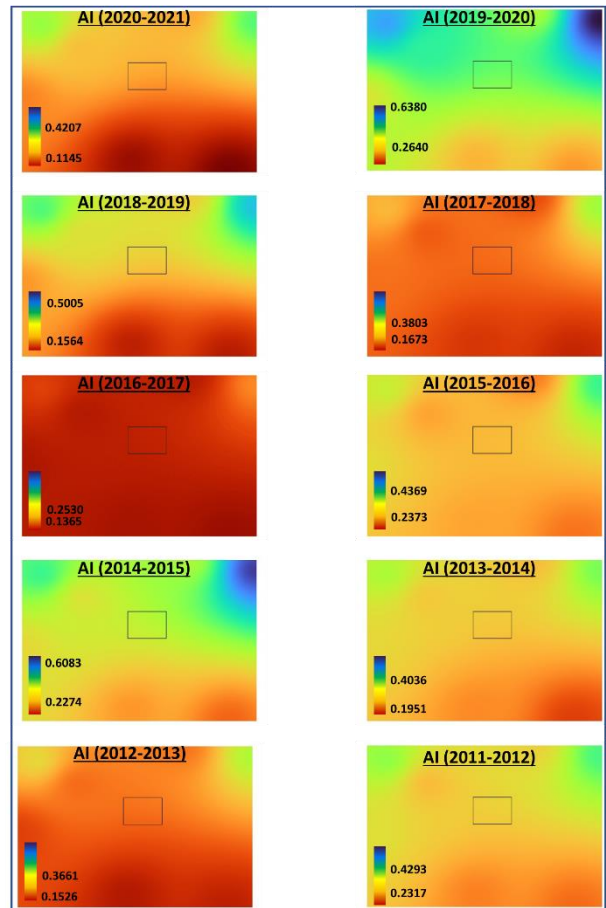
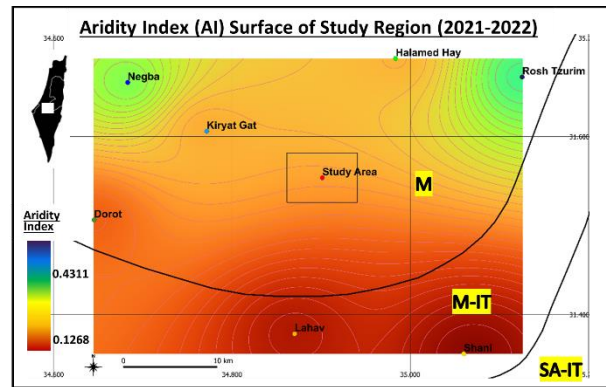


Figure 3. The study area (rectangle) within larger regional chorotype-aridity context derived from interpolation analysis in GIS. Chorotypes M, IT and SA and their combinations after Danin and Orshan (1999: 16) phytogeographical map.

3.4 UAV Vegetation Mapping

Results of the UAV shrub mapping are represented in table 1 according to phanerophyte / chamaephyte species identified in eight microplots during the wet season 2022-2023. 4006 woody plant units were mapped including 3505 phanerophytes and chamaephytes. Percent presence is 64.3% M, 14.3% IT, 14.3% M-IT and 7.1% M-SA with n species = 14 (fig. 4).

Genus species	Name	Raunkiaer	Chorotype	Commonality	Habitat
<i>Pistacia lentiscus</i>	Mastic Bush	Planerophyte	Mediterranean	V. common	Maquis
<i>Rhamnus lycoides</i>	Palmotian Buckthorn	Planerophyte	Mediterranean	V. common	Maquis
<i>Quercus coccifera</i>	Kermes Oak	Planerophyte	Mediterranean	Common	Maquis
<i>Sarcopoterium spinosum</i>	Thorny Burnet	Chamaephyte	Mediterranean	V. common	Garrigue
<i>Bollata undulata</i>	Undulate Horehound	Chamaephyte	Mediterranean	V. common	Garrigue
<i>Chilidactylus iphionoides</i>	Sharp Verbena	Chamaephyte	Mediterranean	V. common	Hard-rock
<i>Micromeria nervosa</i>	Veined Savary	Chamaephyte	Mediterranean	V. common	Hard-rock
<i>Teucrium divaricatum</i>	Aegean Sage	Chamaephyte	Mediterranean	Common	Garrigue
<i>Fumana arabica</i>	Rock Rose	Chamaephyte	Mediterranean	Common	Garrigue
<i>Teucrium capitatum</i>	Cat-thyme Germander	Chamaephyte	Med-Irano-Turanian	V. common	Garrigue
<i>Phagnalon rupestre</i>	African Fleabane	Chamaephyte	Med-Irano-Turanian	V. common	Hard-rock
<i>Phlomis brachydon</i>	Short-tooth Phlomis	Chamaephyte	Irano-Turanian	V. common	Garrigue
<i>Noaea mucronata</i>	Thorny Saltwort	Chamaephyte	Irano-Turanian	Common	Shrub-steppe
<i>Kickxia aegyptiaca</i>	Egyptian toadflax	Chamaephyte	Med-Saharo-Arabian	V. common	Garrigue

Table 1. Results of UAV mapping study in the Gad Hills Nature Reserve. Phanerophytes / chamaephytes reflect presence in the winter 2022/23 based on 5 plant leaf-on minimum.

Very common / common shrub species of the published cross-referenced association (sect. 2.1.3) are defined as 75% M, 15% M-IT, 5% IT, and 5% M-SA with n species = 20. A simple linear regression between the percent presence of the published cross-referenced association and 2022-2023 field survey was conducted and reflects the correlation (p-value = 0.009 and R Square = 0.982). However, any climate change that this reflects must be correlated with aridity, which is discussed in section 3.5.

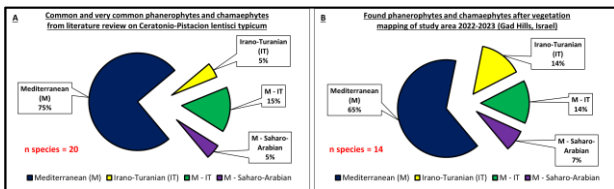


Figure 4. Percent presence of common and very common phanerophytes and chamaephytes by chorotype in the study area: (A) from the published cross-referenced association; and (B) UAV assisted mapping 2022-2023 in Gad Hills, Israel.

The vegetation mapping also provided significant findings regarding the landscape mosaic (Forman, 1995). The microplots represent a mix of garrigue / maquis habitats with a stable patch matrix of phanerophytes and inter-patch chamaephyte species (see fig 5). Based on Raunkiaer type, the phanerophytes are homogenously 100% M chorotype and maquis, while chamaephytes are heterogenously 55% M, 18% M-IT, 18% IT, 9% M-SA and represent garrigue, hard rock, and shrub-steppe habitats. The results demonstrate that light grazing as a proximate cause of arrested succession helps to slow woody encroachment and encourage chamaephyte regeneration. This is important because distinction between phanerophyte and chamaephyte dynamics can help to focus climate change analysis more efficiently by temporal responses. This is also discussed further in section 3.5, although for the purposes of mapping the mosaic, it is crucial to isolate the background phanerophyte matrix from the regenerating chamaephytes. In that way, once the phanerophyte matrix mapping is complete, monitoring the composition change in the LTCMS is dependent on following the inter-patch chamaephyte regeneration over time. The differentiation may distinguish between evergreen sclerophyll phanerophyte and seasonal dimorphic chamaephyte response to climate changes with regard to variability and fluctuation.

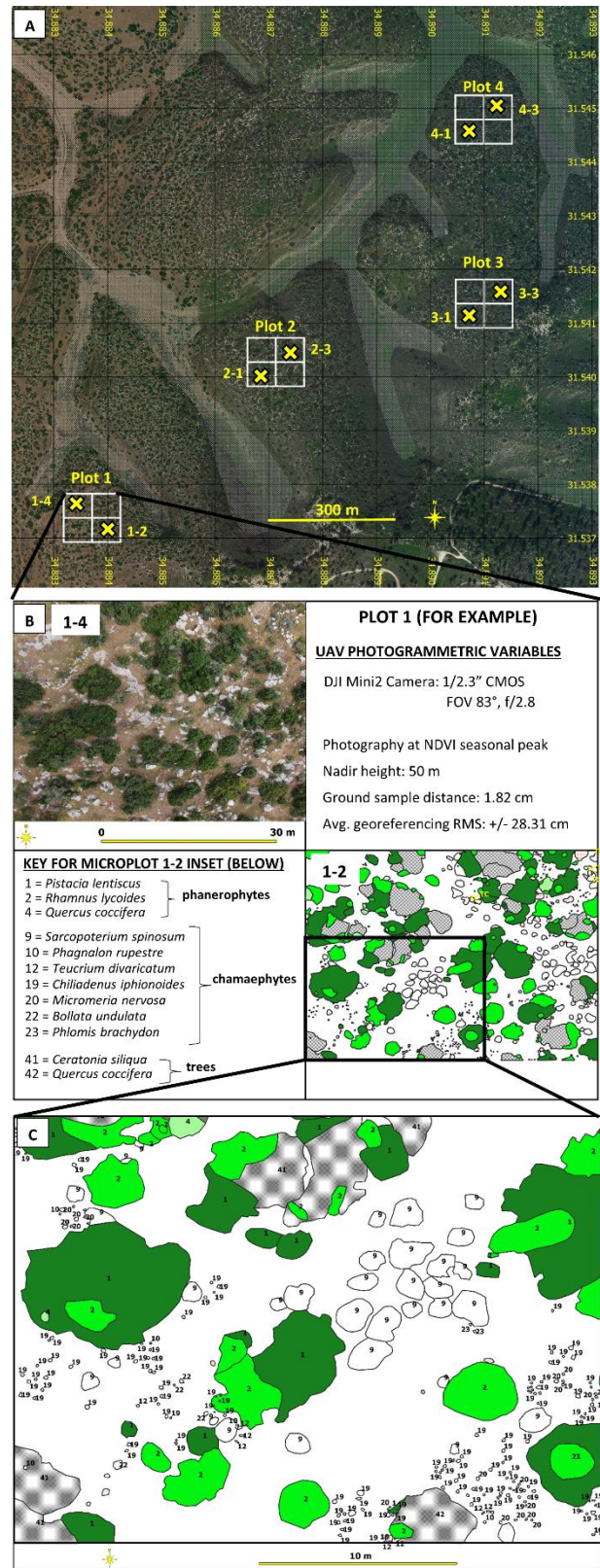


Figure 5. The UAV assisted mapping at scale from (A) the four plots shown on aerial photography; (B) plot 1, for example, with two microplots: microplot 1-4 shown as the UAV nadir photo and microplot 1-2 shown as the digitized product after mapping the vegetation; (C) inset from microplot 1-2, for example, with a legend to demonstrate the phanerophyte matrix with inter-patch chamaephyte species.

3.5 Phytogeographic-Climature correlation

This section summarizes the results of the study and describes the phytogeographic-climate correlation. That is assisted by theorizing biogeographical regions at scale while mapping the floristic association as a geographic field exercise. The study area, within the Tethyan and African floristic subkingdoms, is comprised of three main bioregions, namely M, IT and SA chorotypes (Loidi, 2021; Takhtajan, 1986). This is expressed, in-situ, through vegetation compositions in which the homogenous and mixed chorotypes change over time according to climate conditions. Vegetation is classified according to content of the compositions as percent presence based on plant taxa and units. The unit of the study area has been described as the *Cerantonio-Pistacion lentisci typicum* association or part of the larger class of carob maquis in Israel (Zohary and Orshan, 1959). Following fieldwork in 2022-2023, the study area is currently defined by percent chorotype presence of phanerophytes and chamaephytes as 64.3% M, 14.3% IT, 14.3% M-IT and 7.1% M-SA (fig. 5).

Due to prolonged synanthropic relationship of the area, there are two main interactions between humans and the landscape. The first is the long-term historical LU impact from monoculture agricultural practices that produced a LU legacy in the garrigue / maquis LC. The second is the modern LU of light grazing that holds the current carob maquis from woody encroachment in a state of arrested succession. The grazing enables chamaephyte sub-shrub regeneration between the patches of phanerophyte shrubs that grow there based on the LU legacy. Shrub species may be linked with chorotype and the evolutionary adaptations associated with climate regime at the chorotype geo-origin. This provides indication of the favorable / unfavorable conditions that limit and enable regeneration for each species over time. This notion has been discussed regarding lag times of vegetation in response to climate change (Wu et al., 2015) in which vegetation demonstrates temporal response, positive and negative, to climate conditions. Figure 6 provides a view of this approach as conditions in the study area move between favorable and unfavorable over time relative to chorotype.

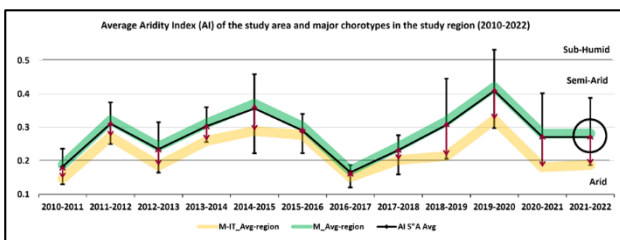


Figure 6. Range of AI in the study area (black line with high-low bars) between M-IT chorotype (yellow line) and M chorotype (green line). Current vegetation mapping circled.

The conditions described are AI values associated with chorotype in the study region. For example, in figure 6, the average M and M-IT AI values were extracted from the spatial range of the chorotypes between 2010-2022. Within that larger region, the conditions in the study area are represented by a range of values (high-low bars) that describe the range of favorable / unfavorable conditions that limit and enable the vegetation composition found there. The results are divided into three: (1) avg AI for M chorotype (2) avg AI for M-IT chorotype; and (3) the range of values between the min study area AI value and max M-IT AI value and the max study area AI value and min M AI value. Favorable / unfavorable conditions in the study area may thus be modeled conducive relatively to the shifting aridity. Where the high bars extend into the wetter M chorotype region there are more favorable conditions for M chorotype species which will

flourish. But, when the low bars extend to the drier M-IT chorotype region, the unfavourable conditions to M species restrict their regeneration but enable dispersal of IT chorotype related species.

Vegetation presence changes relative to the climate conditions which indicates a strong relationship between aridity and floristic composition. UAV assisted mapping of woody perennials at the species level, as presented in this paper, enabled further differentiation in temporal response to climate conditions between phanerophytes and chamaephytes. Based on research in climate gradients, discussed in section 1, phanerophytes and chamaephytes respond differently to climatic pulses. This is evident perhaps in the homogeneity of the phanerophyte matrix in comparison with the heterogeneous inter-patch chamaephytes. To demonstrate how the change in species composition can indicate changes in climate based on aridity, chamaephyte and phanerophyte presence (M and IT chorotypes) was extracted from the two data sets. The published cross-referenced association recorded 3 M related phanerophytes, and 15 M / 4 IT related chamaephytes. The recent mapping recorded 3 M related phanerophytes, and 8 M / 4 IT related chamaephytes. Phanerophyte and IT related chamaephyte presence remained constant while M related chamaephyte presence changed by nearly half since the initial mapping of the *Cerantonio-Pistacion lentisci typicum* association (Zohary and Orshan, 1959).

One explanation may be viewed in figure 6 as the chorotypes shift independently relative to the aridity over time and the vegetation composition in the study area is affected by these conditions. 2010-2011 and 2016-2017 were both years in which the M chorotype aridity dropped to arid conditions that are more conducive to the IT species. These are the unfavourable seasons defined by Raunkiaer and others to describe adaptive strategies in plant life-forms (Danin and Orshan, 1990; Keshet et al., 1990) within a larger evolutionary process. Further knowledge of the range of favorable / unfavorable conditions that limit and enable each species, as well as their geographic ranges, is necessary to clarify how evolutionary adaptations may be associated with climate regime at the chorotype geo-origin. That approach can offer assistance to human related climate change issues by identifying conditions that may also prove limiting over time anthropogenically. The method presented in this paper can lead to scaling up the project successfully, spatially and temporally, through remote sensing platforms and statistical analysis that leads to more conclusive results.

4. CONCLUSION

This methods paper demonstrates that utilization of phytogeographic shrub species in synanthropic conditions as indicators of climate change is meritorious. Thus, floristic association dynamics can continuously be monitored through remote sensing efforts and fieldwork. Those dynamics can indicate the unfavorable or favorable conditions of critical climate changes and inform regarding the human response. We recommend development of a LTCMS in the Gad Hills reserve, Israel, as a prototype for the UN SDG 13 agenda and example for the Mediterranean region. The rigorous scope presented in this paper traverses two complex geographic effects: (1) long and short-term anthropogenic disturbances that have differential effects on LC and the substrate; and (2) notions that vegetation presence is a natural indicator of climate conditions interpretable based on chorotype. Further work intends to examine this disjointed trajectory in more depth because it accurately depicts the nexus in human-environmental relations. Ultimately, the process will be linked to atmospheric circulation models for a greater understanding of climates.

REFERENCES

- Almorox, J., Grieser, J., 2016. Calibration of the Hargreaves–Samani method for the calculation of reference evapotranspiration in different Köppen climate classes. *Hydrology Research*, 47(2), 521-531.
- Dagan, Y., 2006. Archaeological Survey of Israel, Map of Amazyia (109) and Lakhish (98). Israel Antiquities Authority. survey.antiquities.org.il/index_Eng.html#/MapSurvey/18 (30 January 2023).
- Danin, A., Fragman-Sapir, O., 2016. Flora of Israel. flora.org.il/en/en/ (30 January 2023).
- Danin, A., Orshan, G., 1990. The distribution of Raunkiaer life forms in Israel in relation to the environment. *Journal of vegetation science*, 1(1), 41-48.
- Danin, A., Orshan, G. 1999: *Vegetation of Israel* (Vol. 1). Backhuys Publishers, Leiden.
- Di Biase, L., Pace, L., Mantoni, C., Fattorini, S., 2021. Variations in Plant Richness, Biogeographical Composition, and Life Forms along an Elevational Gradient in a Mediterranean Mountain. *Plants*, 10(2090), 1-20.
- FAO, 2023. FAOSTAT, Land-Use. Food and Agriculture Organization of the United Nations (FAO). faostat.fao.org/faostat/en/#data/RL (1 February 2023).
- Forman, R. T., 1995. Some general principles of landscape and regional ecology. *Landscape ecology*, 10, 133-142.
- Foster, D., Swanson, F., Aber, J., Burke, I., Brokaw, N., Tilman, D., Knapp, A., 2003. The Importance of Land-Use Legacies to Ecology. *BioScience*, 53(1), 77-88.
- Giourga, H., Margaris, N., Vokou, D., 1998. Effects of grazing pressure on succession process and productivity of old fields on Mediterranean islands. *Environm. Management*, 22(4), 589-596.
- I.M.S., 2023. Israel Meteorological Service Database Israel Meteorological Service. ims.gov.il/en/data_gov (30 January 2023).
- Karnieli, A., 2003. Natural vegetation phenology assessment by ground spectral measurements in two semi-arid environments. *International Journal of Biometeorology*, 47(4), 179-187.
- Karnieli, A., Gabai, A., Ichoku, C., Zaady, E., Shachak, M., 2002. Temporal dynamics of soil and vegetation spectral responses in a semi-arid environment. *International Journal of Remote Sensing*, 23(19), 4073-4087.
- Keshet, M., Danin, A., Orshan, G., 1990. Distribution of ecomorphological types along environmental gradients in Israel: 1. Renewal bud location and leaf attributes. *Ecologia mediterranea*, 16(1), 151-161.
- Kirk, D. A., Hébert, K., Goldsmith, F. B., 2019. Grazing effects on woody and herbaceous plant biodiversity in northern Tunisia. *PeerJ*, 7, e7296.
- Kloner, A., Sagiv, N., 1989. בתי בד מתקופה ההלניסטית [Maresha: Olive Oil Production in the Hellenistic Period]. *Niqrot Zurim*, 15, 17-65.
- Leach, M., Mearns, R. 1996: *The lie of the land: challenging received wisdom on the African environment*. James Currey Ltd, Oxford.
- Liphshitz, N., Lev-Yadun, S., 1986. Cambial activity of evergreen and seasonal dimorphics around the Mediterranean. *IWA journal*, 7(2), 145-153.
- Loidi, J., 2021: Mapping of Biogeographical Territories: Flora, Vegetation and Landscape Criteria. In F. Pedrotti & E. Box (Eds.), *Tools for Landscape-Scale Geobotany and Conservation* (pp. 21-36). Springer, Cham.
- Manspeizer, N., 2006. The Mediation of a Functional-Aesthetic Landscape in New England: New Braintree, Massachusetts and the Identity of Place. *Middle States Geographer*, 39, 84-92.
- Manspeizer, N., Karnieli, A. 2021. Identification of a long-term land-use legacy in the southern Judean foothills, Israel [Master's Thesis]. Ben Gurion University.
- Manspeizer, N., Karnieli, A., 2023. Isolating phytogeographic shrub indicators through geoarchaeology and exploration of a long-term land-use legacy in Israel for aridity-chorotype climate classification. *Geomorphologie* (pending publication).
- Margaris, N., Giourga, C., Koutsidou, E., 1992. Adaptive strategies of plants dominating phryganic ecosystems. *Ekistics*, 59(356/357), 301-305.
- Ostrom, E., 2001: Decentralization and development: The new panacea. In K. Dowding, Hughes, J., Margetts, H. (Ed.), *Challenges to Democracy. Political Studies Association Yearbook* (pp. 237-256). Palgrave Macmillan, London.
- Sasaki, T., Okayasu, T., Jamsran, U., Takeuchi, K., 2008. Threshold changes in vegetation along a grazing gradient in Mongolian rangelands. *Journal of Ecology*, 96(1), 145-154.
- Schmiedel, U., Dengler, J., Etzold, S., 2012. Vegetation dynamics of endemic-rich quartz fields in the Karoo, South Africa, in response to recent climatic trends. *Journal of Vegetation Science*, 23(2), 292-303.
- SOLPOS, 2023. Solar Position and Intensity, Version 2.0. US-DOE. National Energy Lab. midcdmz.nrel.gov/solpos/solpos.html (30 January 2023).
- Takhtajan, A. 1986: *Floristic regions of the world*. The University of California Press, Berkeley.
- TerrSet, 2017. TerrSet Geospatial Monitoring and Modeling System, Version 18.31. Clark University. clarklabs.org/tererset/ (30 January 2023).
- Tzanopoulos, J., Mitchley, J., Pantis, J., 2005. Modelling the effects of human activity on the vegetation of a northeast Mediterranean island. *Applied Vegetation Science*, 8(1), 27-38.
- United Nations, 2011. Decade for Deserts and the fight against Desertification. United Nations. un.org/en/events/desertification_decade/whynow.shtm 1 (30 January 2023).
- USDA, 2006. Sheep and Goat Handling and Facility Options. US Department of Agriculture, 5. URL available upon request (30 January 2023).
- Vossen, P., 2007. Olive oil: history, production, and characteristics of the world's classic oils. *HortScience*, 42(5), 1093-1100.
- Weber, E., 2009. How Much Wine Can a Small Vineyard Produce? UC Davis Small Vineyard Series 1. URL available upon request (30 January 2023).
- White, P. S., Jentsch, A., 2001. The search for generality in studies of disturbance and ecosystem dynamics. *Progress in botany*, 62, 399-450.
- Wu, D., Zhao, X., Liang, S., Zhou, T., Huang, K., Tang, B., Zhao, W., 2015. Time-lag effects of global vegetation responses to climate change. *Global change biology*, 21(9), 3520-3531.
- Zohary, M., Orshan, G., 1959. The maquis of *Ceratonia siliqua* in Israel. *Vegetatio*, 8(5/6), 285-297.